Hindawi
Journal of Nanomaterials
Volume 2019, Article ID 9257018, 8 pages
https://doi.org/10.1155/2019/9257018

Research Article

Bright Alloy CdZnSe/ZnSe QDs with Nonquenching Photoluminescence at High Temperature and Their Application to Light-Emitting Diodes

Tingting Zhang,[1,2] Xugu Zhang,[2] Peizhi Yang,[1] Jinke Bai,[2] Chun Chang,[2] Xiao Jin,[2] Feng Zhao,[3] Yan Huang,[2] and Feng Li[2]

[1]*Key Laboratory of Advanced Technique and Preparation for Renewable Energy Materials, Ministry of Education, Yunnan Normal University, Kunming 650500, China*
[2]*Jiangxi Engineering Laboratory for Optoelectronics Testing Technology, Nanchang Hangkong University, Nanchang 330063, China*
[3]*School of Chemistry and Chemical Engineering, Jiangxi Science and Technology Normal University, Nanchang 330013, China*

Correspondence should be addressed to Peizhi Yang; pzhyang@hotmail.com and Feng Li; lifengnchu@163.com

Received 2 August 2018; Accepted 10 December 2018; Published 5 March 2019

Guest Editor: P. Kumar

Stable luminance properties are essential for light-emitting devices with excellent performance. Thermal photoluminescence (PL) quenching of quantum dots (QDs) under a high temperature resulting from a surface hole or electron traps will lead to unstable and dim brightness. After treating CdZnSe/ZnSe QDs with TBP, which is a well-known passivation reagent of the anions, the excess Se sites on the surface of the QDs were removed and their PL quantum yields (QYs) was improved remarkable. Furthermore, after TBP treatment, the CdZnSe/ZnSe QDs exhibit no quenching phenomena even at a high temperature of 310°C. The electroluminescent light-mitting diodes based on the QDs with TBP treatment also demonstrated satisfied performance with a maximum current density of 1679.6 mA/cm^2, a peak luminance of 89500 cd/m^2, and the maximum values of EQE and luminescence efficiency are 15% and 14.9 cd/A, respectively. The performance of the fabricated devices can be further improved providing much more in-depth studies on the CdZnSe/ZnSe QDs.

1. Introduction

Colloidal quantum dots (QDs) materials are attracting tremendous interest because of their size- and composition-dependent bandgap, high quantum yields (QYs), and solution-processed method with low cost. These advantages have enabled their extensive use in many fields including display, illumination, photovoltaic, and biosensor. As light converters or emitting layer materials, QDs driven optically or electrically with both high luminescence efficiency and stable luminescence properties are one of the crucial factors for the large-scale commercialization of the QD-based light-emitting diodes (QLEDs). QDs including red, green, and blue emission with QYs~100% have been reported [1–3]. For general displaying or lighting applications, heat originated from the nonradiative transition and the resistance of the electric circuit leads the temperature inside the devices as high as 150 – 200°C, under which photoluminescence (PL) quenching of QDs occurs and the brightness becomes unstable and dim. Intense efforts have been carried out on the mechanism of thermal PL quenching for QDs [4–10]. The extent of PL quenching depends on many factors, including surface composition, structure, ligand, solvent, and temperature [4–6]. At high temperature (RT – 200°C), it has been reported that reversible quenching originates from thermally activated escape of carriers to the surface trap states and/or thermally activated creation of trap states, and irreversible quenching is explained by the thermally induced permanent structural changes which giving rise to trap states [7].

Different types of surface hole and electron traps can be identified by PL decay dynamics coupled with PL quantum yield measurements. To exempt device application from the trouble of PL quenching, many efforts have been carried out to remove the surface defects or middle states for QDs,

so as to obtain the "perfect" QDs, which have near unity PL QYs and a single decay channel for the intrinsic combination of excitons. Generally, luminescence properties of emissive material, excited either optically or electrically, are dominated by their excited states. For colloidal QDs, their excited states are usually described as exciton. Optimal characteristics of an exciton in a quantum dot can be achieved by precise control of both interior crystal and surface structure. Control of interior crystal structure is relatively easy with nearly 30 years of efforts. Surface engineering including shell growth and ligand engineering are usually employed to reduce surface defects, hence boost the PL QYs of the QDs.

As emission materials, II-VI QDs are usually coated with another semiconductor shell with a relatively wide bandgap, and the excited states of the core participate mostly in the light emission [11]. Ternary alloyed QDs can be obtained by means of interfusing binary II-VI QDs with another II element, for example, CdZnS and CdZnSe [12–17]. However, the emission wavelengths of pure core CdZnS or CdZnSe QDs are quite limited (ranging from 400 to 475 nm for CdZnS QDs and from 500 to 620 nm for CdZnSe ones) [3, 13, 17], which restricts their further applications. In our previous work, after introducing a versatile ZnSe shell with a moderate bandgap (2.7 eV) upon the CdZnS and the CdZnSe cores, the emission wavelength of the resulting CdZnS/ZnSe and CdZnSe/ZnSe QDs is extended to the deep-red region (680 nm) [18, 19]. Emission tunable CdZnSe QDs can been achieved by tuning the Cd : Zn ratio by incorporating the control of the reaction time and/or temperature [13, 16]. However, pure core QDs usually suffer from low PL QYs resulted from the abundant surface anions or cations. By coating them with monolayer or multilayer of shells to eliminate the traps, their PL QYs can be enhanced remarkably. [3, 20] Herein, we utilize a high-temperature (300°C) injection for the synthesis of CdZnSe cores and an even higher temperature (310°C) for shell growth to obtain CdZnSe/ZnSe core/shell QDs. After treating with TBP, the resulting QDs exhibited improved PL quantum yields (QYs) and no quenching phenomena even at a high temperature of 310°C. The as-fabricated QDs are also employed as emitting materials to assemble QLEDs, which demonstrated satisfied performance.

2. Experimental Section

2.1. Materials. Cadmium oxide (CdO, 99.99%, powder), zinc acetate ($Zn(Ac)_2$, 99.99%, powder), selenium (Se, 99.99%, powder), 1-octadecene (1-ODE, 90%), tributylphosphine (TBP, 98%), oleic acid (OA, 90%), ethyl alcohol (AR, 99.7%), n-hexane (98%), and acetonitrile (99.5%) were purchased from Aladdin Industrial Corporation. All of the commercial reagents are used as received without further purification.

2.2. Synthesis of CdZnSe QDs. In brief, a mixture of 0.25 mmol CdO, 2.5 mmol $Zn(Ac)_2$, 1 mL OA, and 5 mL 1-ODE loaded in a 50 mL three-neck flask were degassed under vacuum for 30 min and then heated to 120°C with magnetic stirring. When the solution became optically clear, it was heated to 300°C under an N_2 flow and maintained at this temperature for 20 min. Next, Se precursor (S-SUS, 0.2 mmol Se powder suspending in 2 mL 1-ODE) was injected quickly into the hot solution. Eight minutes later, core CdZnSe QDs were synthesized.

2.3. Synthesis of CdZnSe/ZnSe QDs. For the synthesis of CdZnSe/ZnSe QDs, the above resulted solution was heated to a higher temperature of 310°C, at which another S-SUS solution containing 1.5 mmol Se powder and 4 mL 1-ODE was injected drop by drop into the flask in 10 min. The temperature was kept at 310°C for 30 min during which the ZnSe shell grew thicker and thicker. Then, the solution was cooled to room temperature.

2.4. Treating CdZnSe/ZnSe QDs with TBP. 1 mL TBP was injected into the solution followed by magnetic stirring at a speed of 500 rpm for 20 min.

2.5. Purification. The mixture of the above-resulted solution, n-hexane, and acetonitrile with volume ratio of 1 : 1 : 2 was heated to 60°C and kept at this temperature for 3 min. Purified CdZnSe/ZnSe QDs were obtained by repeating the precipitation/dispersion method (8000 rpm, 5 min).

2.6. Device Fabrication. QLEDs were fabricated following the similar procedures reported in [21]. Firstly, indium-tin oxide (ITO) glass substrates were cleaned by using of ultrasonic treatment followed by being dried under a N_2 flow and then etched in a UV ozone for 20 min. Next, they were transferred quickly to a glove box full of argon for the assembling of the device. Both concentrations of O_2 and H_2O in the glove box were required to be below 20 ppm. For the deposition of hole-injection layer, PEDOT:PSS was dissolved in isopropanol, and then the solution was spin-coated onto the substrates at a speed of 3500 rpm for 50 s, and then the substrates were baked for half an hour under 150°C. For the deposition of the hole-transport layer, TFB solution (in chlorobenzene, 8 mg/mL) was spun at a speed of 3000 rpm followed by baking at 150°C for 30 min. Subsequently, CdZnSe/ZnSe QDs (in octane, 18 mg/mL) were spin-coated on the TFB surface at a speed of 2000 rpm for 50 s, and ten minutes later, an emission layer formed. PBO solution (in DMF, 2 mg/ml) was spin-coated at a speed of 4000 rpm and then baked at 120°C for half an hour. For the deposition of electron-injection layer, colloidal ZnO nanocrystals (in ethanol, 40 mg/mL) was then spin-coated at a speed of 2000 rpm for 40 s and then baked at 80°C for another 30 min. Finally, by using of vacuum thermal evaporation at a rate of ~0.1 nm/s under a pressure of 4×10^{-6} kPa, metal Al anodes were deposited. The QLEDs were moved away from the glove box for subsequent measurement after being sealed with UV-curing adhesive and glasses.

2.7. Characterization. The optical properties of the prepared CdZnSe/ZnSe QDs material properties were characterized using a steady-state photoluminescence (PL) spectrophotometer (Cary Eclipse, Varian) and a UV-vis spectrophotometer (Cary 300, Varian). Time-resolved photoluminescence experiments were carried out on a spectrometer (Bruker Optics 250IS/SM) with an intensified charge-coupled device detector (CCD; IStar 740, Andor Tech.). Absolute PL QYs

were tested by an absolute QY test system (Quantaurus-QY C11347-11, Hamamatsu Photonics). The structure of the QDs was characterized by a high-resolution transmission electron microscope (TEM; JEM-2010, JEOL) and an X-ray diffractometer (MiniFlex II X-ray diffractometer, Rigaku). The luminescent and the current–voltage (I–V) properties of the fabricated QLEDs were measured on a spectrometer (Maya 2000 Pro, Ocean Optics) coupling with an integrating sphere (3P-GPS-033-SL, Labsphere, Inc.) and a Keithley 2400 current and voltage source meter.

3. Result and Discussion

3.1. PL Optical Properties and Se-SUS Stoichiometry. During the synthesis process, all the reaction conditions for the preparation of CdZnSe QDs were the same, and CdZnSe/ZnSe QDs with different emission wavelengths ranging from 460 to 640 nm were obtained by changing the stoichiometric of the Se-SUS dropped into the solution. ZnSe shell with different thicknesses here plays the role of not only passivating the surface dangling bonds but also changing the energy band structure, consequently, the emission wavelength of the resulted QDs. The digital photograph of the obtained QD solutions after TBP treatment under irradiation of a UV lamp and the corresponding PL spectra for the solutions are shown in Figures 1(a) and 1(b), respectively. Amounts of dropped Se-SUS, peak wavelengths, and full-width-at-half--maximum (FWHM) of the QDs are given in Table 1. With the amount of Se-SUS increasing gradually from 0.50 mmol to 1.20 mmol, the peak emission of the core/shell QDs shifts to shorter wavelength correspondingly.

Bulk semiconductor materials usually have specific conduction band (CB) and valence band (VB). However, theoretical and existing experimental results have indicated that the band structure for nanomaterials, including QDs, is quite complex. The bandgap of bulk CdSe is 1.74 eV with CB −3.75 eV and VB −5.49 eV and that for bulk ZnSe is 2.69 eV with CB −2.81 eV and VB −5.50 eV. With sizes in quantum confinement regime, their band structures become size-dependent, shape and structure sensitive, and relative to the ligands. Even for core ZnSe and shell ZnSe, they may have different bandgap structures which mean different CB, VB, and bandgaps [11, 22]. Shell ZnSe has a specific VB value of −5.7 eV and a varied CB in the range between −2.4 and −2.83 eV. For core ZnSe materials, both their VB and CB are fluctuant, in the range of −5.64 eV and −5.55 eV and −2.32 eV and −2.62 eV, respectively. The CB and VB for core CdSe materials synthesized under different condition vary around −5.55 eV and −3.1 eV, respectively, with small span [22]. The VB values of shell ZnSe, core ZnSe, and core CdSe are close to each other. The bandgap of an alloy core CdZnSe should be between those of core CdSe and core ZnSe, which will be more close to the later one with abundant Zn precursor during the synthesis. Therefore, the intrinsic structure of CdZnSe/ZnSe enables electrons to localize in the CB of both the core and the shell, so as to holes in VB. Consequently, both the excited states of the shell ZnSe and the core CdZnSe are involved with the light emission, and tuning the emission wavelength by manipulating the shell thickness is possible.

The blueshift of the emission and absorption can be well interpreted by energy level changes induced from the slight lattice strain which increases with the shell growth coated onto the compressible CdZnSe core. Thin ZnSe shell composes less stress on the core CdZnSe, and the lattice strain has less function on changing the energy levels. Therefore, the emission and absorption properties rely more on the intrinsic heterostructures of CdZnSe and ZnSe. The energy difference between the CBs and VBs of the core and the shell decides the optical properties. The red emission with thin shell (0.5 mmol Se) may originate from the intrinsic CB-VB energy difference. A thicker shell (0.75 mmol Se) compresses the CdZnSe and leads to a green emission. Theoretical and experimental results have demonstrated that the electronic energy gap will enlarge under compressive force in zinc blende II-VI semiconductors and narrow when tensile strain [23]. The change of VB can be neglected because lattice strains have little significant influence on it [24]. With the shell growth, thick ZnSe shell composes more compresses on the core, thereby leading to a CB elevation, which finally results in notable blueshifts of PL.

TEM image of CdZnSe/ZnSe QDs is shown in Figure 2(a). Their corresponding high-resolution TEM image and size distribution histograms are inset in Figure 2(a). The CdZ nSe/ZnSe QDs show reasonable narrow size distributions with average diameters of 6.76 nm. To further characterize the structures of CdZnSe and CdZnSe/ZnSe QDs, their crystallographic properties were determined by XRD. The characteristic peaks of zinc blende ZnSe (JCPDS no. 65-7409) are located at 27.5°, 45.6°, and 53.3° and those for bulk CdSe (JCPDS no. 19-0191) are 25.4°, 42.1°, and 49.6°. According to the XRD patterns shown in Figure 2(b), all the characteristic peaks of CdZnSe with double diffraction angles of 26.08°, 44.10°, and 53.3° are located between the zinc blende ZnSe and CdSe bulk materials. This suggests a compositional homogeneity of CdZnSe rather than a mixture of CdS and ZnSe. When ZnSe shells were coated onto the CdZnSe cores, characteristic peaks shift to smaller angles of 26.52°, 44.81°, and 52.55°. This blueshift of the diffraction peaks may result from the enlargement of the lattice constant.

3.2. TBP Treatment and High-Temperature Antiquenching PL Properties. The excited states of colloidal are usually described as exciton, which is a pair of photo- or electrogenerated electron and hole bonded together through Coulomb interaction. Owing to their limited physical size, exciton delocalizes within the entire nanocrystal and is mostly exposed to the physical boundary between the nanocrystal and its ligands/solvent. Therefore, apart from the precise control of the interior crystal structure, management of the surface structure is also needed to achieve optimal characterization for excitons. Here, in our synthesis experiment, Se-SUS precursor is used for the synthesis of alloy CdZnSe and shell growth upon the alloy cores, owing to advantages such as high reactive chemical nature, good conversion rate, no other by-products, and strong operability. For the synthesis of alloy CdZnSe, Zn^{2+} is abundant as the mole ratio of Cd : Zn : Se in the reaction mixture is 1 : 10 : 0.8; hence, the surface of the as-synthesized CdZnSe QDs should be

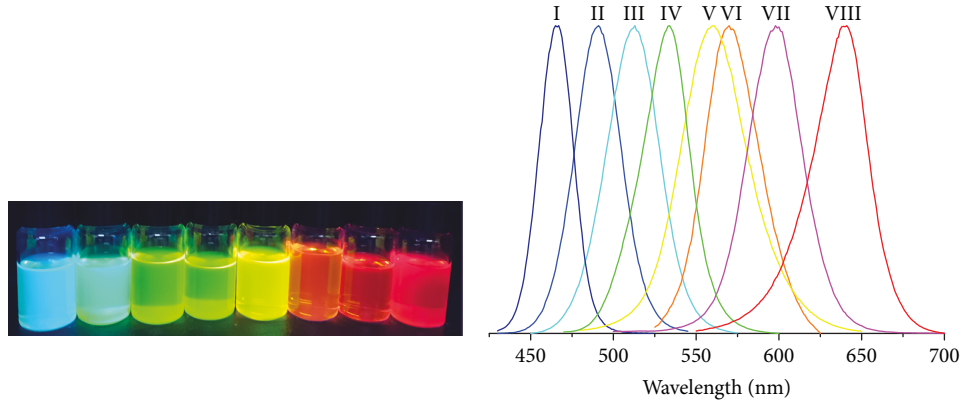

Figure 1: (a) Digital photographs of CdZnSe/ZnSe QD solutions after TBP treatment with different shell thicknesses under the irradiation of a UV lamp. (b) The PL spectra of the obtained CdZnSe/ZnSe QDs.

Table 1: Parameters for the CdZnSe/ZnSe QDs with different emission wavelengths.

Parameter	I	II	III	IV	V	VI	VII	VIII
Se-SUS (mmol)	1.20	1.00	0.80	0.75	0.65	0.60	0.55	0.50
λ_{peak} (nm)	465	490	510	535	560	570	600	640
FWHM (nm)	24	33	38	34	47	39	39	39

cation-rich when the their synthesis is completed. Se-SUS is injected dropwise into the CdZnSe QD solution for the shell growth. With a small amount of Se precursor, thin ZnSe shell grows, Zn^{2+} is still redundant, and the surface of the resulted CdZnSe/ZnSe QDs will still be cation-rich. Cations on the surface have been found to reduce the QY of the radiative decay of excitons. Zn cations can be consumed gradually by increasing of the mole number of Se in Se-SUS, with ZnSe shell getting thicker. With redundant Se-SUS, Zn^{2+} can be depleted, and the surface of the resulting CdZnSe/ZnSe QDs will become anion-rich. However, similar to that of excess cations on the surface of QDs, Se sites will bring hole traps on the QD surface and lead to QY reduction of excitons, or even nearly nonemissive. TBP treatment is a well-known passivation reagent of the Se anions on the surface of CdSe QDs. Upon TBP treatment, the relative PL QY of the final CdZnSe/ZnSe QDs is measured to be 90.9%, much higher than that of the original ones which is 46%.

Absorbance and PL spectra of the as-synthesized CdZnSe, CdZnSe/ZnSe, and TBP-treated CdZnSe/ZnSe QDs are shown in Figure 3(a). Both the absorbance and PL spectra of the CdZnSe/ZnSe and TBP-treated QDs exhibit blueshift, by comparing with to those of the core CdZnSe QDs. The peak wavelength of the as-synthesized CdZnSe QDs is ~555 nm and those of CdZnSe/ZnSe and TBP-treated CdZnSe/ZnSe QDs are ~540 and ~535 nm, respectively, as shown in Figure 3(a). The blueshift of PL of the CdZnSe/ZnSe QDs relative to that of CdZnSe may result from the bandgap change originated from the lattice strain, as described above. The peak emission of TBP-treated CdZnSe/ZnSe QDs also shifts to shorter wavelength slightly, and these small peak wavelength difference between the CdZnSe/ZnSe QDs after and before TBP treatment is attributed to the removal of those "dangling" Se ions on the surface and have been reported in similar QD systems [11].

Many experimental results have identified that anions and cations on the surface induce short and long lifetime channels for the excitons of QDs, respectively. Transient photoluminescence measurements were taken to identify the lifetime of the excitons for cation-rich, anion-rich, and TBP-treated CdZnSe/ZnSe QDs, respectively, their corresponding PL decay spectra are shown in Figure 3(b). The PL QYs and lifetimes for these QDs are also summarized and inset in Figure 3(b). For cation-rich CdZnSe/ZnSe QDs, their PL decay curve can be fitted with one slow channel, ~45 ns, along with the original channel at ~11.43 ns. These results suggested that excess cations on the surface of QDs create shallow electron traps with relatively long lifetime. However, different from cation-rich QDs, the PL decay curve for anion-rich CdZnSe/ZnSe QDs can be fitted with one fast channel, ~4.16 s, along with the original channel at ~9.93 s. The appearance of fast channels usually implies the existence of middle-gap states, and such middle-gap states should efficiently trap the holes and quench the PL. Evidently, the TBP treatment could boost the PL QY to near unity to ~90% for CdZnSe/ZnSe QDs and convert their PL decay dynamics to be nearly monoexponential with a goodness-of-fit of $\chi^2 = 1.12$. Owning to the good intersolubility between the TBP and Se, the excess Se on the surface can be removed efficiently; consequently, the surface defects can be eliminated completely. As a result, the intrinsic decay channel of the excitons of CdZnSe/ZnSe QDs could be nearly completely radiative.

Thermal activated photoionization can cause luminescence quenching because of the escape of a charge carrier from luminescence center. Therefore, surface states, defects, or impurities surrounding the QD can act as trapping centers and lead to the sharp decrease of PL intensity with temperature above RT, which is also known as the luminescence quenching behavior of QDs. Both the solutions of CdZnSe cores and CdZnSe/ZnSe QDs, before and after TBP

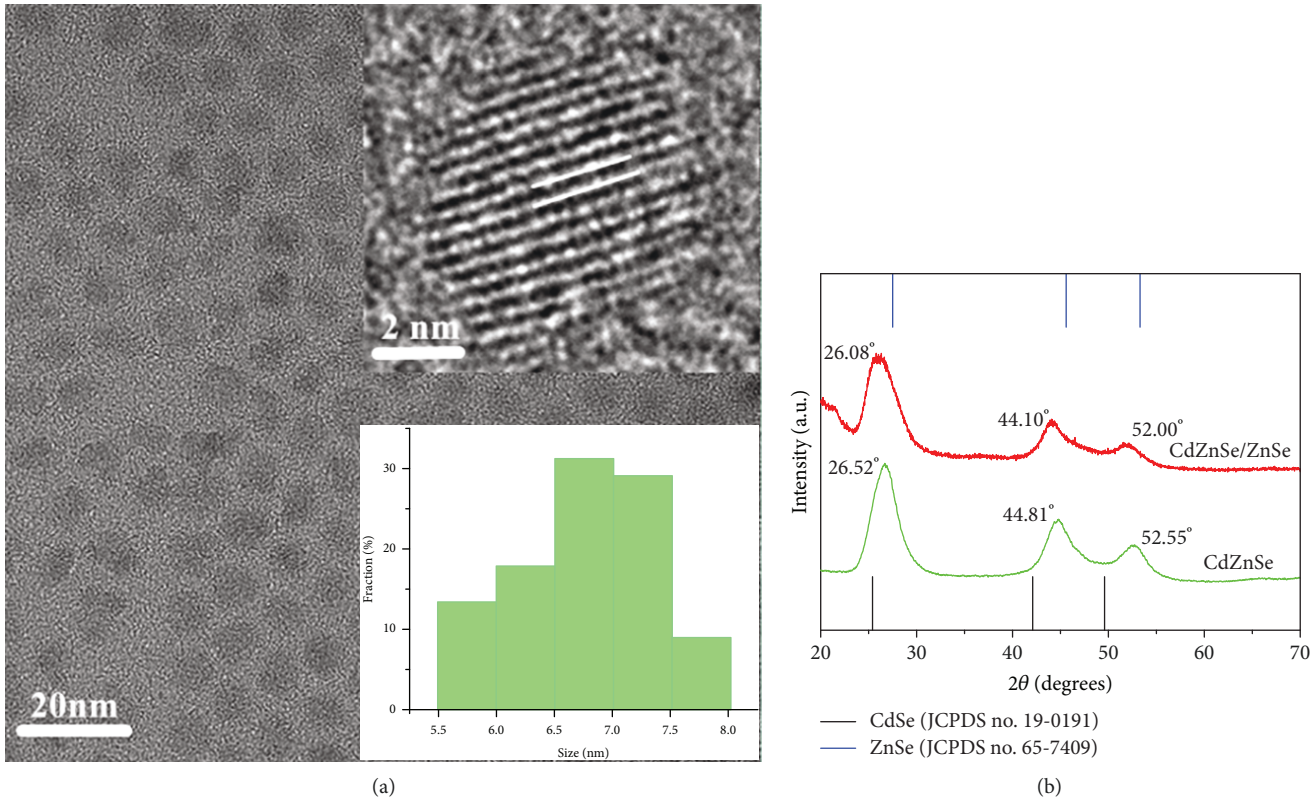

Figure 2: TEM images of (a) CdZnSe/ZnSe QDs and (b) XRD patterns of the CdZnSe core and the CdZnSe/ZnSe QDs. Insets in (a) are the HR-TEM image and the histograms of the size distribution of the CdZnSe/ZnSe QDs, respectively.

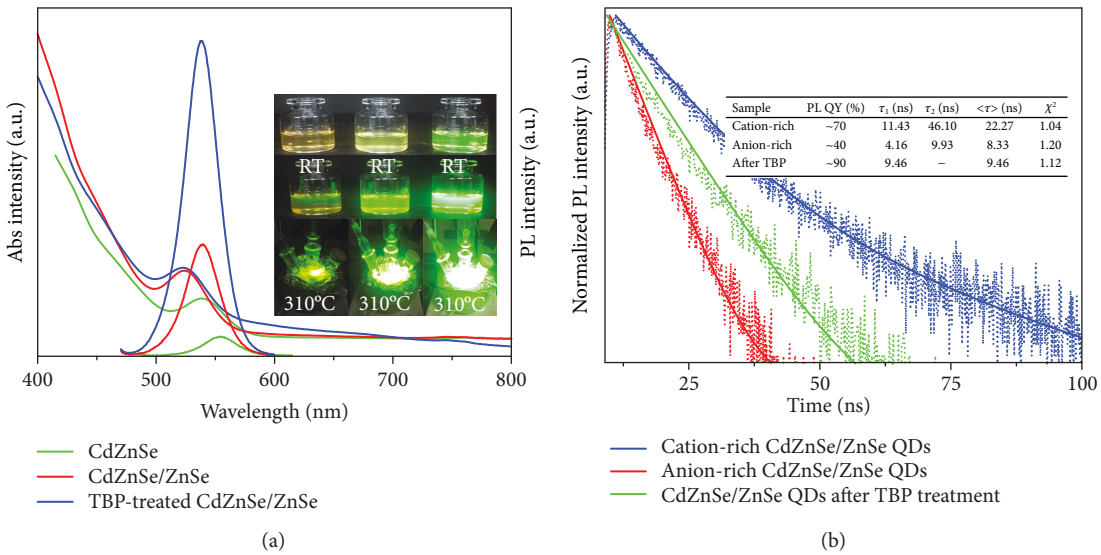

Figure 3: (a) Absorbance and PL spectra for the core CdZnSe QDs and the CdZnSe/ZnSe QDs without and with TBP treatment. (b) PL decay cures for the cation-rich, anion-rich, and the TBP-treated CdZnSe/ZnSe QDs. The photograph's insets in (a) are for the core CdZnSe QDs (left column) and CdZnSe/ZnSe QDs before (middle column) and after TBP treatment (right column) taken under the sunlight at RT (top row), under the UV radiation at RT (middle row), and under the UV radiation at the temperature of 310°C (bottom row), respectively.

treatment, were cooled down to RT and then reheated to 310°C, under which their photographs were taken under UV irradiation and shown in Figure 3. As described above, CdZnSe cores were synthesized at 300°C, and they have cation-rich surface because the total amounts of Cd and Zn are much more than that of Se in the reaction. Middle states resulted from the combination of excess ions on the surface and the ligand detachment occurred at an elevated

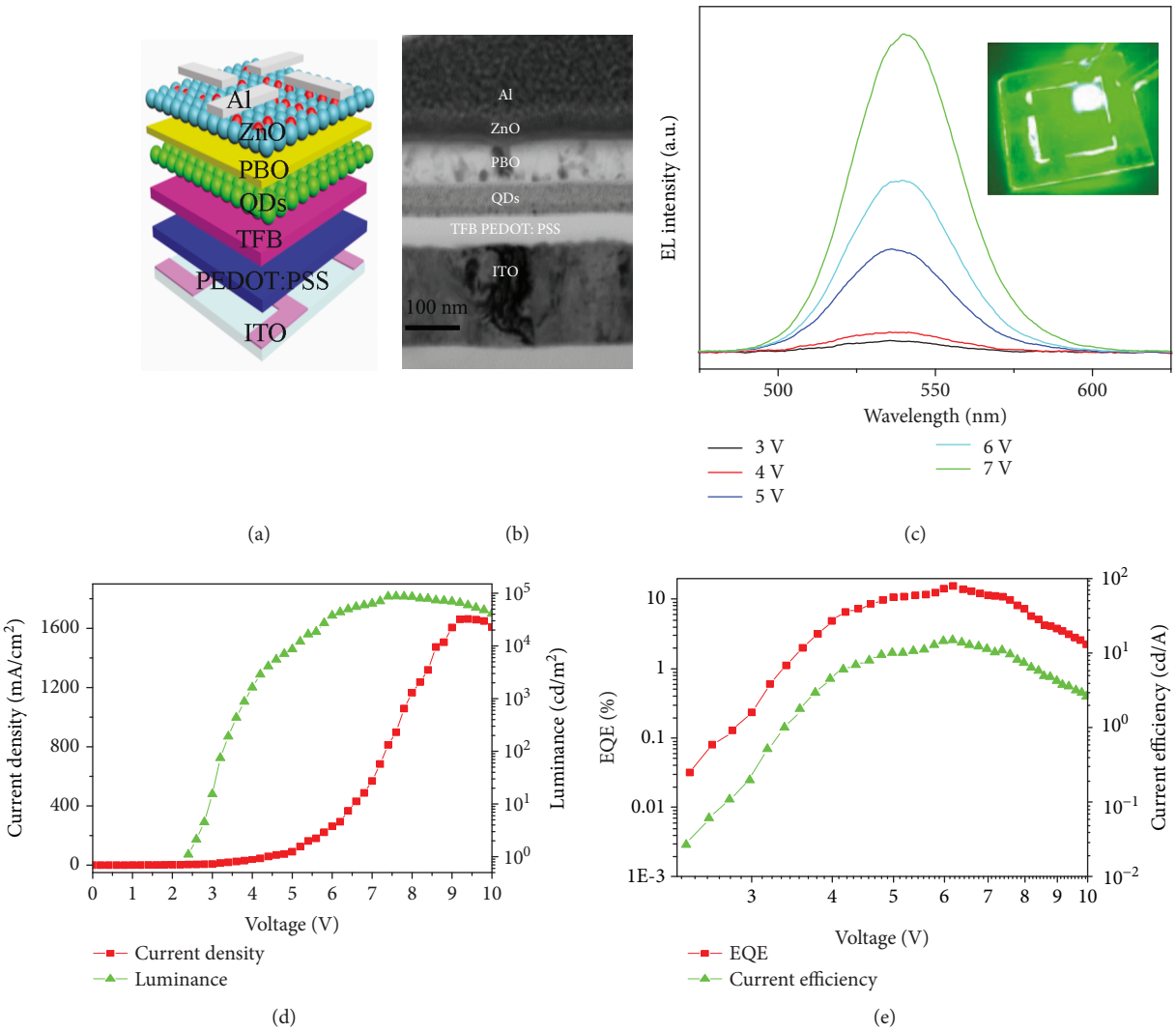

Figure 4: (a) Structure diagram and (b) TEM image of the cross-section of the QLED. (c) EL evolution with increasing applied voltage, and the inset is a luminescent image of the device at 6 V. (d) Variation of current density and luminance with applied voltage. (e) Variation of external quantum efficiency and current efficiency with applied voltage.

temperature probably diminish the PL intensities and reduced the PL QYs of the plain core CdZnSe QDs. Therefore, the luminescence of the CdZnSe QDs looks dim among these three photos, as shown in Figure 3(a). It seems that the luminescence of the CdZnSe/ZnSe QDs before TBP-treatment is brighter than that of core CdZnSe QDs, as shown in Figure 3(a). This is because the abundant Se precursor dropped in flask for shell growth neutralizes the excess cations completely and suppresses the surface middle states somewhat. After TBP treatment, all the excess Se ions on the surface can be removed, so that there are no middle states in the forbidden gaps of QDs, which has been verified by its single-exponential PL decay curve. Therefore, the CdZnSe/ZnSe QDs after TBP treatment exhibit the brightest luminescence among these three QD solutions at the high temperature of 310°C.

3.3. Device Performance. The prepared CdZnSe/ZnSe QDs peaked at ~540 nm are employed as light-emitting materials to assemble QLEDs. The devices have a multilayer structure of ITO/PEDOT:PSS/TFB/QDs/PBO/ZnO/Al, as the structure diagram shown in Figure 4(a). It can be seen from the cross-sectional TEM image of the prepared device shown in Figure 4(b) that the interface of PEDOT:PSS and TFB is almost undistinguishable because both organic polymer films with small thickness are transparent. The electroluminescence (EL) spectra of the device are measured with voltage varying from 3 to 7 V and stacked in Figure 4(c). With the applied voltage increasing, the relative intensity of the EL curve rises steadily while the FWHMs remain almost the same (~40 nm). Furthermore, the redshift of peak emission of the electroluminescent QLEDs often occurs owing to the temperature rise resulting from an increasing voltage or current, which has been reported. However, with applied voltage increasing from 4 to 10 V, the redshift of the EL spectra of the QLEDs based on $CuInS_2$/ZnS QDs is distinguishable [21]. Here, the EL of our devices also shows a slightly perceptible redshift, as can be seen from Figure 4(b). These results

indicate again the good thermal stability of our CdZnSe/ZnSe QDs to some extent.

The current density and luminance of the devices based on the CdZnSe/ZnSe QDs with TPB treatment as a function of driving voltage is shown in Figure 4(d), while the external quantum efficiency η_{EQE} and current efficiency η_A as a function of voltage are shown in Figure 4(e). The device exhibits a low turn-on voltage of approximately 2 V. The current density of the device begins to increase rapidly with driving voltage above 5 V, and it exhibits a maximum value of 1679.6 mA/cm^2 at 9.2 V. The maximum luminance of the device achieves 89500 cd/m^2 at 7.6 V. When the applied voltage is 6.2 V, the EQE achieves to a peak value ~15% and that of luminescence efficiency is 14.9 cd/A. To some extent, the performance of this device indicates that CdZnSe/ZnSe QDs with TBP treatment are suitable for the fabrication of electroluminescent QLEDs with stable luminescent properties.

4. Conclusions

In summary, we synthesized CdZnSe/ZnSe QDs with unable emission wavelength covering most part of the visible range. "Perfect" CdZnSe/ZnSe QDs with a near-unity PL QY of 90.6% also obtained by means of TBP treatment and transient PL analysis on their PL decay curve proved that their exciton radiates through a single decay intrinsic channel. When these QD solutions were heated to a high temperature of 310°C, nonquenching behavior was observed. Green-emission CdZnSe/ZnSe QDs were also employed as active material to fabricate QLEDs which also exhibit satisfied luminescent performance. These results indicate that CdZnSe/ZnSe QDs after TBP treatment are promising candidate materials for the fabrication of light-emitting devices.

Data Availability

The data used to support the findings of this study are included within the article.

Conflicts of Interest

The authors declare that there is no conflict of interest regarding the publication of this paper.

Acknowledgments

The authors gratefully acknowledge financial supports from the National Natural Science Foundation of China (NSFC) (U1802257, 11564026, and 21563013); the Key Applied Basic Research Program of Yunnan Province (Grant No. 2017FA024); the Program for Innovative Research Team (in Science and Technology) of the Yunnan University; the Natural Science Foundation of Jiangxi Province (2018 1BAB201016 and 20181BAB202028); the Outstanding Youth Funds of Jiangxi Province (20171BCB23052); and the Science and Technology Project of the Education Department of Jiangxi Province (GJJ170582 and GJJ170591).

References

[1] C. Pu, H. Qin, Y. Gao, J. Zhou, P. Wang, and X. Peng, "Synthetic control of exciton behavior in colloidal quantum dots," *Journal of the American Chemical Society*, vol. 139, no. 9, pp. 3302–3311, 2017.

[2] S. Jun and E. Jang, "Bright and stable alloy core/multishell quantum dots," *Angewandte Chemie International Edition*, vol. 52, no. 2, pp. 679–682, 2013.

[3] H. Shen, X. Bai, A. Wang et al., "High-efficient deep-blue light-emitting diodes by using high quality $Zn_xCd_{1-x}S$/ZnS core/shell quantum dots," *Advanced Functional Materials*, vol. 24, no. 16, pp. 2367–2373, 2014.

[4] Y. X. Zhang, H. Y. Wang, Z. Y. Zhang et al., "Photoluminescence quenching of inorganic cesium lead halides perovskite quantum dots ($CsPbX_3$) by electron/hole acceptor," *Physical Chemistry Chemical Physics*, vol. 19, no. 3, pp. 1920–1926, 2017.

[5] P. Dutta and R. Beaulac, "Photoluminescence quenching of colloidal CdSe and CdTe quantum dots by nitroxide free radicals," *Chemistry of Materials*, vol. 28, no. 4, pp. 1076–1084, 2016.

[6] X. Cai, J. E. Martin, L. E. Shea-Rohwer, K. Gong, and D. F. Kelley, "Thermal quenching mechanisms in II–VI semiconductor nanocrystals," *Journal of Physical Chemistry C*, vol. 117, no. 15, pp. 7902–7913, 2013.

[7] Y. Zhao, C. Riemersma, F. Pietra, R. Koole, C. de Mello Donegá, and A. Meijerink, "High-temperature luminescence quenching of colloidal quantum dots," *ACS Nano*, vol. 6, no. 10, pp. 9058–9067, 2012.

[8] A. Shi, J. Sun, Q. Zeng et al., "Photoluminescence quenching of CdTe/CdS core-shell quantum dots in aqueous solution by ZnO nanocrystals," *Journal of Luminescence*, vol. 131, no. 7, pp. 1536–1540, 2011.

[9] P. Jing, J. Zheng, M. Ikezawa et al., "Temperature-dependent photoluminescence of CdSe-Core CdS/CdZnS/ZnS-multishell quantum dots," *Journal of Physical Chemistry C*, vol. 113, no. 31, pp. 13545–13550, 2009.

[10] D. Valerini, A. Cretí, M. Lomascolo, L. Manna, R. Cingolani, and M. Anni, "Temperature dependence of the photoluminescence properties of colloidal CdSe/ZnS core/shell quantum dots embedded in a polystyrene matrix," *Physical Review B*, vol. 71, no. 23, p. 235409, 2005.

[11] Y. Gao and X. Peng, "Photogenerated excitons in plain core CdSe nanocrystals with unity radiative decay in single channel: the effects of surface and ligands," *Journal of the American Chemical Society*, vol. 137, no. 12, pp. 4230–4235, 2015.

[12] X. Zhong, Y. Feng, W. Knoll, and M. Han, "Alloyed $Zn_xCd_{1-X}S$ nanocrystals with highly narrow luminescence spectral width," *Journal of the American Chemical Society*, vol. 125, no. 44, pp. 13559–13563, 2003.

[13] X. Zhong, M. Han, Z. Dong, T. J. White, and W. Knoll, "Composition-tunable $Zn_xCd_{1-X}Se$ nanocrystals with high luminescence and stability," *Journal of the American Chemical Society*, vol. 125, no. 28, pp. 8589–8594, 2003.

[14] Y. C. Li, M. F. Ye, C. H. Yang, X. H. Li, and Y. F. Li, "Composition- and shape-controlled synthesis and optical properties of $Zn_xCd_{1-x}S$ alloyed nanocrystals," *Advanced Functional Materials*, vol. 15, no. 3, pp. 433–441, 2005.

[15] Y.-M. Sung, Y.-J. Lee, and K.-S. Park, "Kinetic analysis for formation of $Cd_{1-x}Zn_xSe$ solid-solution nanocrystals," *Journal of*

the American Chemical Society, vol. 128, no. 28, pp. 9002-9003, 2006.

[16] S. R. Chung, K. W. Wang, and H. S. Chen, "Green light emission of $Zn_xCd_{1-x}Se$ nanocrystals synthesized by one-pot method," *Journal of Nanomaterials*, vol. 2013, Article ID 526862, 9 pages, 2013.

[17] S.-R. Chung, K.-W. Wang, H.-S. Chen, and H.-H. Chen, "Novel red-emission of ternary ZnCdSe semiconductor nanocrystals," *Journal of Nanoparticle Research*, vol. 17, no. 2, p. 101, 2015.

[18] F. Li, L. You, C. Nie et al., "Quantum dot white light emitting diodes with high scotopic/photopic ratios," *Optics Express*, vol. 25, no. 18, pp. 21901–21913, 2017.

[19] Q. Zhang, C. Nie, C. Chang et al., "Highly luminescent red emitting CdZnSe/ZnSe quantum dots synthesis and application for quantum dot light emitting diodes," *Optical Materials Express*, vol. 7, no. 11, pp. 3875–3884, 2017.

[20] Y. Niu, C. Pu, R. Lai et al., "One-pot/three-step synthesis of zinc-blende CdSe/CdS core/shell nanocrystals with thick shells," *Nano Research*, vol. 10, no. 4, pp. 1149–1162, 2017.

[21] F. Li, C. Guo, R. Pan et al., "Integration of green $CuInS_2$/ZnS quantum dots for high-efficiency light-emitting diodes and high-responsivity photodetectors," *Optical Materials Express*, vol. 8, no. 2, pp. 314–323, 2018.

[22] K. V. Vokhmintcev, P. S. Samokhvalov, and I. Nabiev, "Charge transfer and separation in photoexcited quantum dot-based systems," *Nano Today*, vol. 11, no. 2, pp. 189–211, 2016.

[23] H. Maki, T. Sato, and K. Ishibashi, "Direct observation of the deformation and the band gap change from an individual single-walled carbon nanotube under uniaxial strain," *Nano Letters*, vol. 7, no. 4, pp. 890–895, 2007.

[24] Y.-H. Li, X. G. Gong, and S.-H. Wei, "*Ab initio* all-electron calculation of absolute volume deformation potentials of IV-IV, III-V, and II-VI semiconductors: the chemical trends," *Physical Review B*, vol. 73, no. 24, article 245206, 2006.